

Antenna Count for Massive MIMO: 1.9 GHz versus 60 GHz

Larsson, E. G., Marzetta, T. L., Ngo, H. Q., & Yang, H. (2018). Antenna Count for Massive MIMO: 1.9 GHz versus 60 GHz. *IEEE Communications Magazine*, 56(9), 132-137. <https://doi.org/10.1109/MCOM.2018.1700526>

Published in:
IEEE Communications Magazine

Document Version:
Peer reviewed version

Queen's University Belfast - Research Portal:
[Link to publication record in Queen's University Belfast Research Portal](#)

Publisher rights
© 2019 IEEE.

This work is made available online in accordance with the publisher's policies. Please refer to any applicable terms of use of the publisher.

General rights

Copyright for the publications made accessible via the Queen's University Belfast Research Portal is retained by the author(s) and / or other copyright owners and it is a condition of accessing these publications that users recognise and abide by the legal requirements associated with these rights.

Take down policy

The Research Portal is Queen's institutional repository that provides access to Queen's research output. Every effort has been made to ensure that content in the Research Portal does not infringe any person's rights, or applicable UK laws. If you discover content in the Research Portal that you believe breaches copyright or violates any law, please contact openaccess@qub.ac.uk.

ANTENNA COUNT FOR MASSIVE MIMO: 1.9 GHz VERSUS 60 GHz

Erik G. Larsson, Linköping University, Linköping, Sweden
 Thomas L. Marzetta, New York University, NY, USA
 Hien Quoc Ngo, Queen's University, Belfast, U.K.
 Hong Yang, Nokia Bell-Labs, Murray Hill, NJ, USA

Abstract

If we assume line-of-sight propagation and perfect channel state information at the base station – consistent with slow moving terminals – then a direct performance comparison between Massive MIMO at PCS and mmWave frequency bands is straightforward and highly illuminating. Line-of-sight propagation is considered favorable for mmWave because of minimal attenuation, and its facilitation of hybrid beamforming to reduce the required number of active transceivers.

We quantify the number of mmWave (60 GHz) service antennas that are needed to duplicate the performance of a specified number of PCS (1.9 GHz) service antennas. As a baseline we consider a modest PCS deployment of 128 antennas serving 18 terminals. At one extreme, we find that, to achieve the same per-terminal max-min 95%-likely downlink throughput in a single-cell system, 20000 mmWave antennas are needed. To match the total antenna area of the PCS array would require 128000 half-wavelength mmWave antennas, but a much reduced number is adequate because the large number of antennas also confers greater channel orthogonality. At the other extreme, in a highly interference-limited multi-cell environment, only 215 mmWave antennas are needed; in this case, increasing the transmitted power yields little improvement in service quality.

1 Introduction

Massive MIMO [1] and millimeter-wave (mmWave) communications [2–7] are the two main physical-layer techniques considered for wireless access in 5G and beyond. The relative merits of one over the other have been the subject of much public debate, most recently, in the Globecom 2016 industry panel “Millimeter wave versus below 5 GHz Massive MIMO: Which technology can give greater value?”. The object of this paper is to give some insight into the relative performances of the two technologies in a scenario where uncontested models of the physical propagation channels exist: line-of-sight between the terminals and the base station(s), and negligible terminal mobility.

1.1 Massive MIMO Below 5 GHz

Massive MIMO relies on the use of large antenna arrays at the base station. In TDD operation, each base station learns the uplink channel responses from its served terminals through measurements of uplink pilots. By virtue of reciprocity of propagation, these estimated responses are valid also in the downlink. Based on the estimated channels, the base station performs multiuser MIMO decoding on uplink and precoding on downlink. In FDD operation, in contrast, downlink pilots and subsequent feedback of channel state information from the terminals are required.

Fundamentally, the permitted mobility is dictated by the dimensionality of the channel coherence interval – that is, the coherence bandwidth in Hertz multiplied by the coherence time in seconds. In a TDD deployment, the coherence interval determines how many terminals may be multiplexed, because all terminals must be assigned mutually orthogonal pilot sequences that fit inside this coherence interval. In an FDD deployment, the coherence interval dimension limits both the number of base station antennas (as each antenna needs to transmit a downlink orthogonal pilot) and the amount of channel state information that each terminal can report.

Frequency bands below 5 GHz are particularly attractive for TDD Massive MIMO, because they support aggressive spatial multiplexing under high terminal mobility, as proven both by information-theoretic calculations [1] and by practical experiments [8]. In addition, below 5 GHz diffraction is significant and electromagnetic waves penetrate non-metallic objects and foliage well – enabling the coverage of wide areas both indoors and outdoors.

1.2 mmWave Communications

Millimeter Wave communications typically refers to wireless operations in the band between 30 and 300 GHz. Its feasibility has been demonstrated in practice, for example, using beam-tracking algorithms in a small-cell environment [9] and highly directive horn antennas for transmission in rural areas [10]. The technology is considered a contender for the provision of outdoor cellular access [5, 7].

Compared to sub-5 GHz bands, the physics at mmWave bands is different in several respects:

1. The effective area of an antenna, for a constant gain pattern, scales in proportion to $1/f_c^2$, where f_c is the carrier frequency. This means that for a given radiated power, the number of receiver antennas required to maintain a predetermined link budget scales proportionally to f_c^2 . Consequently, either numerically big arrays, or directive antenna elements, are needed to facilitate transmission over large distances.
2. mmWaves do not penetrate solid objects well, and propagation is dominated by the pres-

ence of unobstructed direct paths and specular reflection. Thus, the conditions favorable to mmWave entail either line-of-sight, or a few reflections.

3. The Doppler frequency is proportional to the carrier frequency, implying increasing difficulty in acquiring channel state information for high mobility terminals.

Fortunately, as the propagation becomes increasingly line-of-sight, the acquisition of complete channel responses, for the purpose of precoding and decoding, is not necessary. The identification of a line-of-sight path, potentially combined with a few reflected paths, is sufficient in order to obtain channel estimates that are sufficiently accurate.

It may be questioned whether spatial multiplexing to a large number of users is relevant for mmWave communications, since such systems usually cover relatively small cells. However, future applications may very well require the service of much greater densities of terminals at much higher data rates as compared to today. Examples that are discussed currently include virtual and augmented reality, and transmission of uncompressed real-time imagery and video (for machine learning purposes) for example between vehicles and infrastructure (V2X).

Indeed, it is frequently stated that mmWave is favorable for Massive MIMO multiplexing because the small size of each antenna permits the deployment of numerically large arrays in a small space. This argument has been accepted uncritically, in the absence of analyses regarding how many antennas would actually be required.

1.3 The Role of Bandwidth

An argument in favor of mmWave communications is the availability of huge bandwidths. While this is certainly correct, extreme bandwidth is only useful if there is an available reserve of effective power. Specifically, by the Shannon-Hartley formula, capacity scales as $B \log_2(1 + P/(BN_0))$, where B is the bandwidth in Hertz, P is the received power in Watt, and N_0 is the noise spectral density in Watt/Hertz. The capacity is an increasing function of B , for fixed P . However, the returns of increasing B are diminishing: if $B \rightarrow \infty$ for fixed P , then the capacity approaches a *finite* limit equal to $(P/N_0) \log_2(e)$.

As an example, suppose that nominally 10 Watt of radiated power over a bandwidth of 20 MHz is required to sustain a rate of 60 Mbps. If the bandwidth is increased 50 times, to 1 GHz, then in order to also achieve a 50-fold increase in capacity, the radiated power must be increased 50 times, to 500 Watt. If a smaller capacity increase can be accepted, less power is required. For example, suppose that with a 50-fold increase in bandwidth, a mere 25-fold increase in rate is satisfactory. Then the required radiated power over 1 GHz bandwidth is only 131 Watt.

The attractiveness of extreme bandwidth is further diminished because it reduces the signal-to-noise ratio (SNR) of received pilot signals, and consequently degrades the quality of the channel

estimates. Let $\rho_0 = P/(B_0 N_0)$ be the SNR that occurs for some reference bandwidth B_0 . Then the throughput (for sufficiently high bandwidth) is approximately $B \log_2(1 + \rho_0 B_0^2/B^2)$, so at some point, additional bandwidth results in smaller throughput. This holds irrespective of whether the bandwidth is used to serve one terminal, or whether several terminals are orthogonally multiplexed in different parts of the band. This “squaring effect” that results when channel estimates are obtained from uplink pilots is explained in more detail in [1, Chap. 3]. Only if the channel estimates are obtained from a parametric model (e.g., estimation of direction-of-arrivals), then the throughput scaling with B can be more favorable.

2 Sub-5 GHz versus mmWave Comparison

To maintain a constant power-aperture product with increasing carrier frequency would require the number of antennas to grow with the square of the carrier frequency. However, the increasing number of antennas facilitates spatial multiplexing because of greater channel orthogonality, so some reduction in the power-aperture product is permissible. Specifically, the probability that two channel responses are similar decreases sharply when increasing the number of antennas in the array. This results in a new, intriguing tradeoff, if the multiplexing of many simultaneous terminals is of interest, and the provision of uniformly good quality of service in the cell is of concern. Nominally, considering only the path loss, $(60/1.9)^2 \approx 1000$ times more antennas would be required at mmWave (60 GHz) as compared PCS (1.9 GHz) to maintain the same link budget – implying, that 128000 mmWave antennas would be required to match 128-antenna PCS. While this is an important conclusion per se, there is also a countervailing effect: in a scenario where many terminals are spatially multiplexed, the PCS system may be at a disadvantage because its smaller number of antennas renders it much more likely that some terminal must be dropped from service due to channel non-orthogonality. Thus, the proportionate number of extra antennas required for the mmWave carrier may be considerably smaller than 1000. This effect is particularly pronounced under line-of-sight conditions [1, Section 7.2.3].

The following discussion will quantitatively address this point, and specifically the question: For a predetermined quality-of-service, how many more antennas will a mmWave system require, compared to the PCS system?

2.1 Single Cell

We first consider a single Massive MIMO cell, in which a circular base station array, comprising M antennas at half-wavelength ($\lambda/2$) spacing (Figure 1) serves a multiplicity of terminals, randomly located in the cell. The array diameter (aperture) is $d = M\lambda/(2\pi)$. A number of terminals are placed uniformly at random inside the cell, and multiplexed simultaneously in the same time-frequency resource.

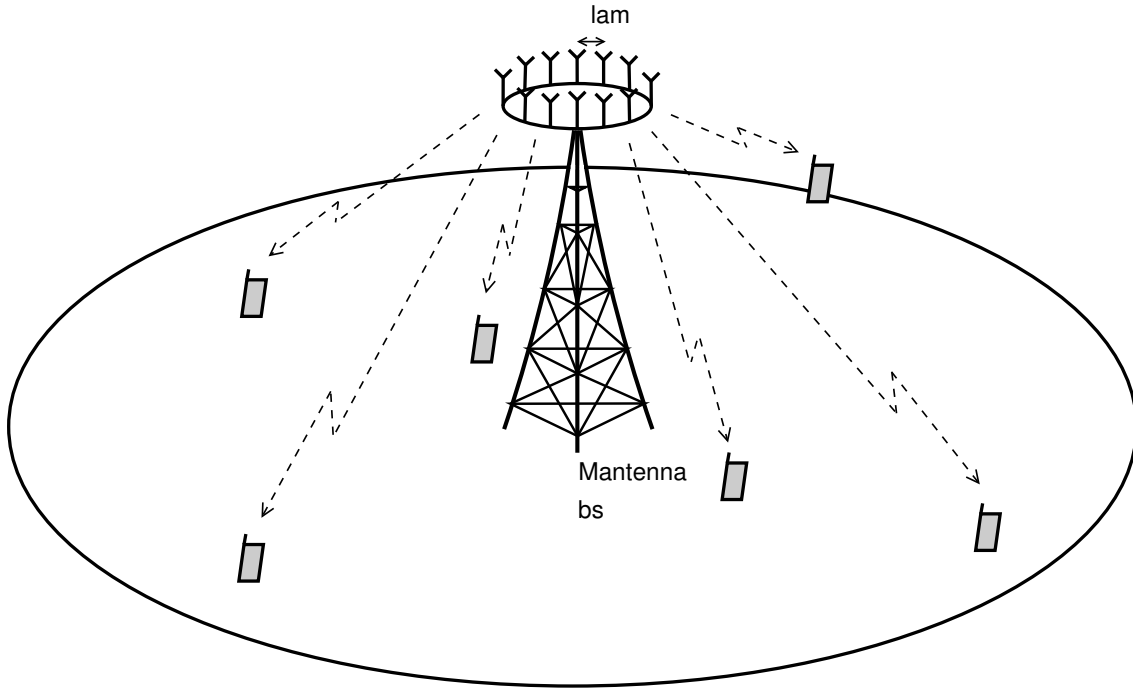


Figure 1: Single cell with circular base station array and line-of-sight to all terminals. The base station equipped with M antennas (half-wavelength spacing) simultaneously serves multiple single-antenna terminals. All terminals are located uniformly at random inside the cell.

There is line-of-sight between the base station antennas and the terminals. The assumption of LoS propagation is, in fact, realistic for some scenarios (large crowds of people in a stadium, for example, or in Times Square, New York). Non-line-of-sight operation would hurt mmWave more than PCS. In addition, a rich scattering environment would further hamper the use of hybrid (part analog, part digital) beamforming schemes for mmWaves – the only hope for reducing the huge number of active antenna circuits. Note also that in line-of-sight, Friis' free-space propagation equation holds exactly, facilitating analysis without reliance on empirical path loss models.

There is negligible mobility. This enables the base station to learn the channel responses with arbitrarily good accuracy, and it makes outage capacity a legitimate performance measure. This assumption also, substantially, eliminates the distinction between TDD and FDD mode operation.

We focus on this scenario, because of its simplicity and ease of analysis, and because, if anything, it is biased in favor of mmWave. Any departure from line-of-sight propagation would create more difficulties for mmWave than for PCS. Likewise, any terminal mobility would require the expenditure of significant resources on channel estimation, to the greater detriment

Number of simultaneously multiplexed terminals	18
Distribution of terminal locations	uniform within circular cell
Cell radius	250 m
Base station height over ground	30 m
Propagation model	line-of-sight (Friis free-space equation)
Base station antenna element gain	0 dBi
Terminal antenna gain	0 dBi
Power control	max-min SINR fairness (uniform quality-of-service)
Bandwidth	50 MHz
Terminal height over ground	1.5 m
Base station radiated power (downlink)	2 W
Terminal radiated power (uplink)	200 mW
Base station noise figure	9 dB
Terminal noise figure	9 dB

Table 1: Massive MIMO system parameters.

of mmWave because of its 30-times larger Doppler frequency. Notwithstanding, this may be a realistic model for, again, operation in a stadium or in Times Square.

The base station performs zero-forcing (ZF) decoding and precoding, which is known to be more effective than maximum-ratio (MR) decoding and precoding for obtaining effective signal-to-noise-and-interference ratios (SINRs) significantly greater than one [1]. Also, under line-of-sight propagation, there is a significant chance for high non-orthogonality between channels, which is precisely where ZF is effective [11]. Efficient hardware implementations have been demonstrated for reasonably-sized systems [12]. Max-min power control ensures that every terminal enjoys the same effective SINR [1, 11].

The random location of each terminal induces a random path-loss. Standard Massive MIMO analysis techniques yield an SINR – and an accompanying lower bound on the achievable rate – for each terminal, in terms of the path loss and the power control coefficients. In turn, the power control coefficients are chosen according to the max-min criterion, as described in [1, Chap. 5] and [11]. A repetition of the procedure for many independent realizations of terminal location yields an empirical cumulative distribution for the max-min SINR.

Table 1 quantitatively summarizes all relevant parameters used in this case study. We adopt isotropic antenna gains of 0 dBi solely for simplicity. A more realistic model would, of necessity, have directional dependence which would introduce additional random components to the propagation, e.g., the orientation of the terminal antenna. Owing to the no-mobility assumption, the choice of duplexing (TDD or FDD) is immaterial.

Figure 2 shows the cumulative probability distribution of the effective SINR on uplink and downlink, for the PCS and the mmWave systems. All randomness originates from the random terminal locations. The PCS system has 128 antennas and the mmWave system has 20000 antennas. In Figure 2, the 95%-likely downlink SINR (the point at cumulative probability 0.05 in the plots – approximately 38 dB) is comparable for both systems. The mmWave system has 156 times more antennas than the PCS system. This is substantially less than predicted by a path-loss analysis $((60/1.9)^2 \approx 1000 \text{ times})$. The reason is the improved orthogonality conferred by the larger number of antennas at mmWaves. This improved orthogonality is also reflected by the increased steepness of the curves.

Table 2(a) shows the required number of base station antennas, and the corresponding array diameter, for different 95%-likely uplink SINRs. The mmWave array comprises a fairly large number of antennas but is geometrically rather compact. On downlink, fewer antennas are required in either case (not shown in the table).

The following remarks are in order:

1. The 95%-likely SINR targets in Table 2(a) range from moderate to very high. From a purely information-theoretic point of view, for a given SINR, $\log_2(1 + \text{SINR})$ bits/s/Hz could be achieved. However, for the high SINR values, the resulting modulation scheme would require large constellation sizes and therefore may be sensitive to phase noise.
2. There is no interference, neither within the cell (owing to the perfect-CSI assumption), nor from other cells (owing to the single-cell assumption).
3. Hypothetically, if all channels were orthogonal and all terminals were subject to the same path loss, the uplink-downlink SINR difference would be equal to the power imbalance between uplink and downlink, $(18 \times 0.2)/2 = 1.8 \approx 2.6 \text{ dB}$. Considering the path loss differences and given that we use max-min power control, most of the terminals do not expend full power in the uplink. However, full power is expended and shared among all terminals in the downlink. So the power imbalance between uplink and downlink will be smaller than 2.6 dB. This is evident in Figure 2 (the mmWave curves) where the channels are nearly orthogonal for large numbers of service antennas.

With far fewer antennas, the PCS channels are far less orthogonal. The advantage of power pooling in the downlink is seen in Figure 2 (the PCS curves).

4. The quantitative results are somewhat pessimistic since the max-min fairness power control criterion forces the simultaneous service of every terminal in the cell with the same SINR. If two terminals are located close to one another (with nearly the same direction-of-arrivals), then the resulting channel is ill-conditioned and much power needs be expended to invert it. Better performance could be obtained by scheduling one of those terminals

on an orthogonal resource (for example, a different subcarrier), or a much reduced level of service.

However, numerical experiments not disclosed here have shown that this effect is rather minor. Also, importantly, the effect is much larger for small numbers of base station antennas. Hence, insofar a required-number-of-antennas comparison is concerned, the inclusion of an orthogonal scheduling option would favor the PCS system much more than the mmWave system.

5. The use of antennas with larger physical aperture (i.e., intrinsic directivity) would not change the conclusions, because such use of directional antennas is essentially equivalent to sectorization. The problem is that to exploit the intrinsic gain, the antennas must *a priori* point into a given direction. Consequently, in the array, only a subset of the antennas will be useful when serving a particular terminal. This negatively impacts both the resulting channel gain (in terms of reduced effective aperture, since only few of the antennas point into the direction of a randomly selected terminal) and – importantly – the channel orthogonality (see, e.g, Chapter 7 in [1]).
6. The array geometry can have a large impact on the performance. Figure 3 illustrates this point quantitatively, by comparing a rectangular, a linear, and a circular array for the uplink. The circular array significantly outperforms the other two. The reason is that neither the rectangular nor the linear array has any resolution capability in its endfire directions. Similar observations hold for the downlink (not shown in Figure 3).
7. The mmWave system may utilize multiple antennas more readily at the terminals, resulting in a received power gain, as well as interference nulling capabilities. This is possible also in the PCS system, but antenna arrays at the terminals will be bulkier.
8. The mmWave system may have access to much larger bandwidths, although correspondingly higher radiated powers are required to efficiently exploit these bandwidths – as discussed above.
9. Achieving high SNR requires array diameters on the order of 1 to 3 meters. While this physical size is substantial, nothing prevents such antenna arrays from being engineered. Traditional arrays could be constructed using metallic frames, or antennas could be mounted on pre-existing buildings, concrete structures or steel frames. Yet, we speculate that more advantageously, structures may be built from modern materials (e.g., carbon-fiber reinforced polymer) with physically small antenna elements, cables and all required electronics integrated inside.
10. The mmWave array is certainly smaller than the PCS array, but the maximum ratio of diameters is far smaller than the wavelength ratio of 32.

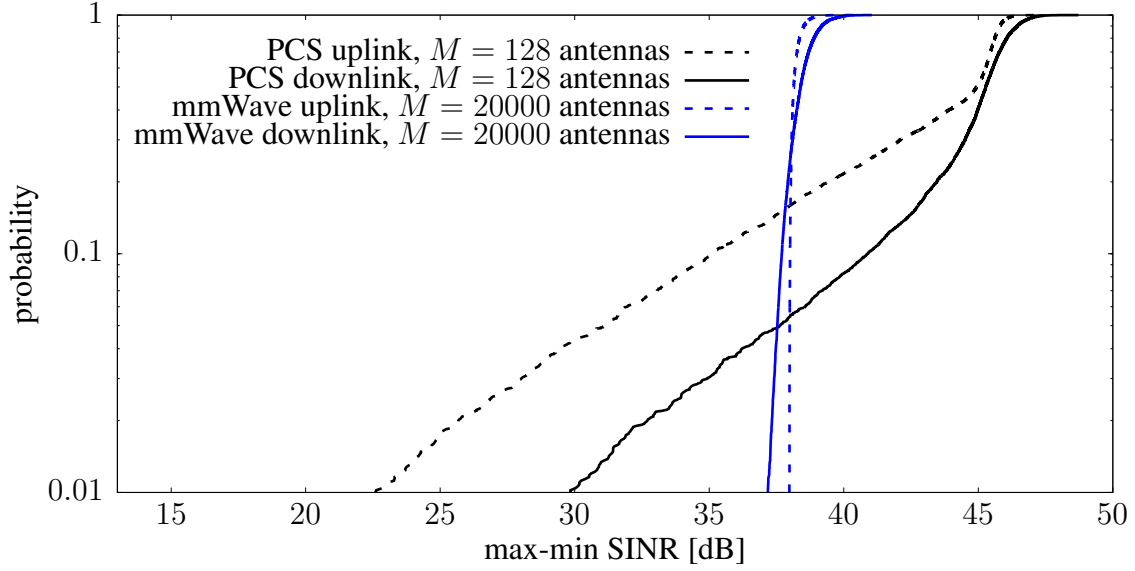


Figure 2: Uplink and downlink SINR in the PCS ($f_c = 1.9$ GHz) respectively mmWave ($f_c = 60$ GHz) systems, for a single-cell deployment.

11. Some savings in mmWave electronics may be realized by employing hybrid beamforming that exploits the structure of line-of-sight propagation [13]. Yet, the angle spread associated with non-line-of-sight propagation will limit the extent to which hybrid beamforming may be used.
12. Non-line-of-sight propagation would cause signals to attenuate at a rate much greater than in free space, with mmWave more disadvantaged than PCS. Our line-of-sight analysis ignores the sensitivity of mmWave signals to blockage. Blockage by the human body alone can yield tens of dB of losses [14]. A possible remedy to that problem is to establish coverage from multiple access points.
13. The zero-mobility assumption, and the consequent unlimited coherence time, makes our scenario very favorable for mmWave technology. In reality, channel estimation and/or beam training will be required. These tasks are more challenging for mmWave technology, since the channels change at thirty times the rate of PCS channels.

Table 2(b) summarizes similarities and differences between PCS and mmWave Massive MIMO.

2.2 Multiple Cells

A legitimate question is whether the above single-cell example is too “extreme” and to what extent the conclusions would change in a multi-cell environment. Naturally, the salient fea-

95%-likely max-min SINR	Required number of antennas (M)		Array diameter (meter)	
	PCS (1.9 GHz)	mmWave (60 GHz)	PCS (1.9 GHz)	mmWave (60 GHz)
5 dB	33	160	0.83	0.13
10 dB	40	250	1.0	0.20
15 dB	54	360	1.4	0.29
20 dB	64	560	1.6	0.45
25 dB	90	1100	2.3	0.87
30 dB	110	4000	2.8	3.2

(a) Number of antennas, and resulting diameter of the circular array, required to obtain a given 95%-likely uplink SINR, for the single-cell setup.

	PCS	mmWave
spectrum available for 5G	some new	much new
market value of spectrum	U.S. operators paid \$40 billion for 65 MHz in 2014	not known
required M	some 100	some 10000
uniform quality-of-service (max-min power control)	feasible within a cell, regardless of propagation [1]	feasible within a cell, if line-of-sight (this paper)
probability that two channels are considerably correlated	small	very small
mobility	handles well	very challenging (30× Doppler)
blocking (e.g. by human body)	not a problem	serious issue
nature of interference (in environment with mobility)	stationary	non-stationary

(b) Similarities and differences between PCS and mmWave Massive MIMO.

Table 2: Comparison between Massive MIMO at PCS and mmWave frequency bands.

tures of PCS versus mmWave operation are at work fully in the single-cell scenario. However, in a multi-cell system, intercell interference may become significant and eventually the main limiting factor.

A proper multi-cellular analysis would require many additional assumption to be made (all subject to controversy), including the selection of appropriate terminal-to-base station assignment

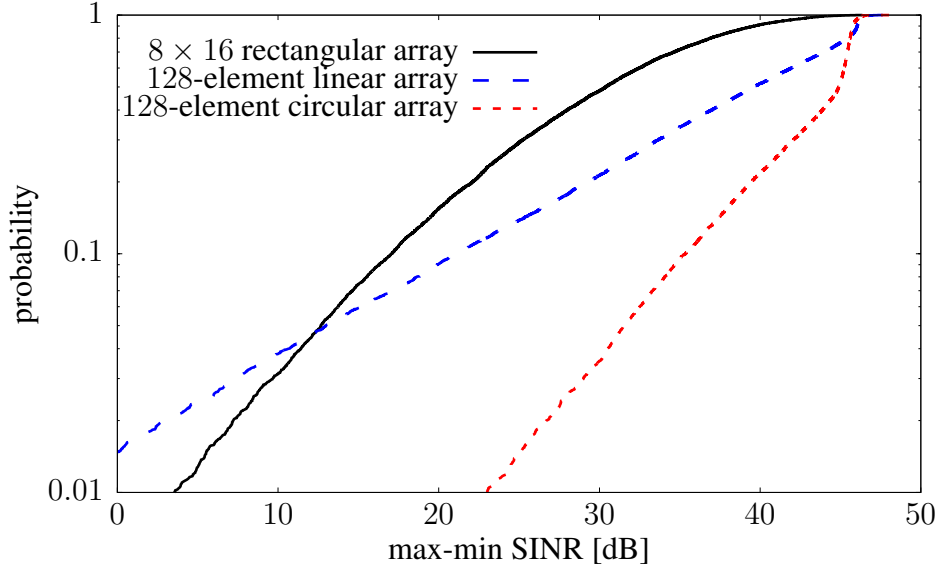


Figure 3: Uplink SINRs for different array geometries, in the single-cell case and for the PCS system. In the rectangular and linear arrays, the distance between neighboring elements is $\lambda/2$. In the circular array, the arc distance between neighboring antennas is $\lambda/2$.

algorithms and power control schemes. In particular, while max-min fairness power control is feasible *within a cell*, equalization of the throughputs *over multiple cells* is not scalable, so heuristic schemes are required that achieve fairness between the different cells. While these issues are rather well understood for PCS systems under an independent Rayleigh fading assumption (see, e.g., [1, Chaps. 5–6]), they are not well investigated for mmWave systems. In particular, modeling of intercell interference is non-trivial at mmWaves, first, because that interference is likely to be non-stationary, and second, because even though propagation within the cell is line-of-sight, interference from other cells may not be.

Notwithstanding, the effects of intercell interference can be illustrated through simple modeling. To examine the effect to its extreme, we consider a system with seven neighboring circular cells, using system-wide max-min fairness power control, and assume that there is line-of-sight propagation between all base stations and terminals. This results in an extremely interference-limited scenario. Figure 4 shows the corresponding results. In this setup, a 128-antenna PCS system offers roughly equivalent performance to a 215-antenna mmWave system. Due to the high amount of intercell interference, here the power advantage of PCS becomes relatively unimportant. This is why much fewer mmWave antennas are required to make up the power disadvantage.

Note that under the adopted negligible-mobility model, perfect channel state information is available at the base station and then interference on the pilot channels becomes a non-issue.

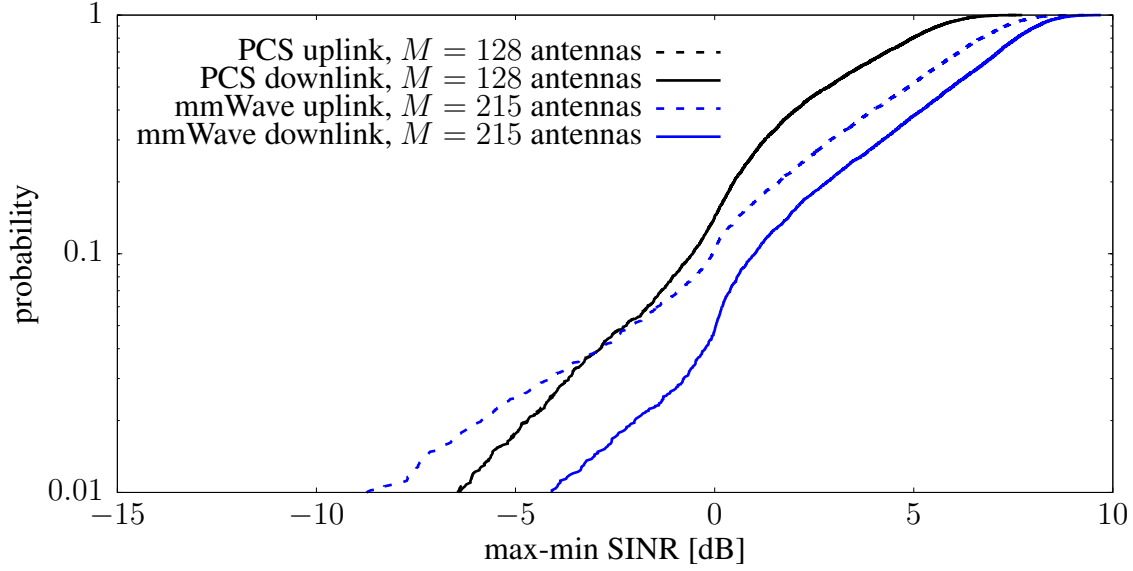


Figure 4: Uplink and downlink SINR in the PCS respectively mmWave systems, for a multi-cell deployment with line-of-sight between all base stations and all terminals, no blocking, and system-wide max-min fairness power control. The uplink and downlink curves for PCS overlap in the plot.

Consequently, in a multi-cell environment only non-coherent interference is present, whose magnitude is independent of the number of base station antennas.

3 Discussion and Conclusions

The main message is that when increasing the number of base station antennas, the channel orthogonality improves. While a link budget analysis would predict that a factor $(f_2/f_1)^2$ more antennas are required when going from a carrier frequency f_1 to a carrier frequency f_2 , in reality that number can be much smaller. While previous work exists [15] that has addressed the question of relative performance between different carrier frequencies, the point on channel orthogonality – which proves to be exceedingly important in context – has not been articulated elsewhere to our knowledge.

Notwithstanding, in a noise-limited environment (the single-cell example), the number of antennas required to compensate for a decreased effective antenna area can be quite large. Specifically, for a particularly simple scenario – line-of-sight propagation and perfect CSI – we compared 128-antenna PCS (1.9 GHz) massive MIMO with mmWave (60 GHz):

- For a noise-limited single-cell setup, a link budget calculation might predict that $128 \times$

$(60/1.9)^2 \approx 128000$ mmWave antennas are needed to match the performance of 128-antenna PCS MIMO, but there is a countervailing effect in that increasing the number of antennas improves channel orthogonality so that only 20000 antennas are required.

- In contrast, in a severely interference-limited multi-cell scenario, the numbers of antennas required at the two different carrier frequencies are comparable (128 versus 215). In this interference-limited regime, the power advantage of PCS becomes unimportant and the performance becomes independent of the carrier frequency.

4 Acknowledgements

The authors thank the Swedish research council (VR) and ELLIIT for funding parts of this work.

References

- [1] T. L. Marzetta, E. G. Larsson, H. Yang, and H. Q. Ngo, *Fundamentals of Massive MIMO*. Cambridge University Press, 2016.
- [2] S. Rangan, T. S. Rappaport, and E. Erkip, “Millimeter-wave cellular wireless networks: Potentials and challenges,” *Proceedings of the IEEE*, vol. 102, no. 3, pp. 366–385, Mar. 2014.
- [3] T. S. Rappaport, R. W. Heath Jr., R. C. Daniels, and J. N. Murdock, *Millimeter Wave Wireless Communications*. Pearson Education, 2014.
- [4] T. S. Rappaport, S. Sun, R. Mayzus, H. Zhao, Y. Azar, K. Wang, G. N. Wong, J. K. Schulz, M. Samimi, and F. G. Jr., “Millimeter wave mobile communications for 5G cellular: It will work!” *IEEE Access*, vol. 1, pp. 335–349, May 2013.
- [5] W. Roh, J.-Y. Seol, J. Park, B. Lee, J. Lee, Y. Kim, J. Cho, K. Cheun, and F. Aryanfar, “Millimeter-wave beamforming as an enabling technology for 5G cellular communications: theoretical feasibility and prototype results,” *IEEE Commun. Mag.*, vol. 52, no. 2, pp. 106–113, 2014.
- [6] A. L. Swindlehurst, E. Ayanoglu, P. Heydari, and F. Capolino, “Millimeter-wave massive MIMO: the next wireless revolution?” *IEEE Commun. Mag.*, vol. 52, no. 9, pp. 56–62, 2014.
- [7] J. G. Andrews, T. Bai, M. N. Kulkarni, A. Alkhateeb, A. K. Gupta, and R. W. Heath, “Modeling and analyzing millimeter wave cellular systems,” *IEEE Trans. Commun.*, vol. 65, no. 1, pp. 403–430, 2017.

- [8] P. Harris, S. Malkowsky, J. Vieira, F. Tufvesson, W. B. Hassan, L. Liu, M. A. Beach, S. Armour, and O. Edfors, “Performance characterization of a real-time massive MIMO system with LOS mobile channels,” *IEEE J. Sel. Areas Commun.*, pp. 1244–1253, Jun. 2017.
- [9] V. Raghavan, “QualComm demonstration at IEEE Globecom 2016,” private communication.
- [10] G. R. MacCartney, Jr., S. Sun, T. S. Rappaport, Y. Xing, H. Yan, J. Koka, R. Wang, and D. Yu, “Millimeter wave wireless communications: new results for rural connectivity,” in *Proc. Workshop on All Things Cellular - Operations, Applications and Challenges, ATC@MobiCom, New York, USA*, Oct. 2016, pp. 31–36.
- [11] H. Yang and T. L. Marzetta, “Massive MIMO with max-min power control in line-of-sight propagation environment,” *IEEE Trans. Commun.*, vol. 65, pp. 4685–4693, Nov. 2017.
- [12] H. Prabhu, J. Rodrigues, L. Liu, and O. Edfors, “A 60 pJ/b 300 Mb/s 128 x 8 massive MIMO precoder-detector in 28 nm FD-SOI,” in *International Solid-State Circuits Conference (ISSCC)*, 2017.
- [13] O. E. Ayach, S. Rajagopal, S. Abu-Surra, Z. Pi, and R. W. Heath, Jr., “Spatially sparse precoding in millimeter wave MIMO systems,” *IEEE Trans. Wireless Communications*, vol. 13, no. 3, pp. 1499–1513, Mar. 2014.
- [14] S. Collonge, G. Zaharia, and G. E. Zein, “Influence of the human activity on wide-band characteristics of the 60 GHz indoor radio channel,” *IEEE Trans. Commun.*, vol. 3, no. 6, pp. 2396–2406, 2004.
- [15] R. W. Heath, Jr., “Comparing massive MIMO and mmWave MIMO,” Talk at the IEEE Communication Theory Workshop, 2014.

5 Biographies

Erik G. Larsson is Professor at Linköping University, Sweden. He co-authored *Fundamentals of Massive MIMO* (Cambridge, 2016) and *Space-Time Block Coding for Wireless Communications* (Cambridge, 2003). Recent service includes membership of the IEEE Signal Processing Society Awards Board (2017–2019), and the *IEEE Signal Processing Magazine* editorial board (2018–2020). He received the IEEE Signal Processing Magazine Best Column Award twice, in 2012 and 2014, the IEEE ComSoc Stephen O. Rice Prize in Communications Theory 2015, the IEEE ComSoc Leonard G. Abraham Prize 2017 and the IEEE ComSoc Best Tutorial Paper Award 2018. He is a Fellow of the IEEE.

Thomas L. Marzetta is Distinguished Industry Professor in the ECE Department at NYU Tandon School of Engineering. He joined NYU in 2017 after spending thirty-nine years in three industries: petroleum exploration, defense, and telecommunications. He is the originator of Massive MIMO. Recognition for his achievements includes the IEEE Communications Society Industrial Innovation Award, the IEEE Stephen O. Rice Prize, the IEEE W. R. G. Baker Award, and the Honorary Doctorate from Linköping University.

Hien Quoc Ngo received his Ph.D. in 2015 from Linköping University, Sweden. He is now an assistant professor at Queen's University Belfast, U.K. His research interests are the applications of mathematical, statistical, random matrix, optimization theories, and signal processing to wireless communications. He received the IEEE ComSoc Stephen O. Rice Prize in 2015, the IEEE ComSoc Leonard G. Abraham Prize in 2017, and the Best Ph.D. Award from EURASIP in 2018.

Hong Yang received the Ph.D. degree in applied mathematics from Princeton University, USA. He is a member of technical staff with the Mathematics of Networks and Communications Research Department, Nokia Bell Labs, Murray Hill, NJ, USA, where he conducts research in communications networks. He has coauthored many research papers in wireless communications, applied mathematics, control theory, and financial economics. He coined many U.S. and international patents. He coauthored the book *Fundamentals of Massive MIMO*.